Creating a Multi-material Probing Error Test for the Acceptance Testing of Dimensional Computed Tomography Systems

Borges de Oliveira, Fabrício; Stolfi, Alessandro; Bartscher, Markus; Neugebauer, Michael

Published in:
Proceedings of the 7th Conference on Industrial Computed Tomography (iCT 2017)

Publication date:
2017

Document Version
Publisher's PDF, also known as Version of record

Creating a Multi-material Probing Error Test for the Acceptance Testing of Dimensional Computed Tomography Systems

Fabricio Borges de Oliveira[1], Alessandro Stolfi[2], Markus Bartscher[1], Michael Neugebauer[1]

[1]Physikalisch-Technische Bundesanstalt, Bundesallee 100, 38116 Braunschweig, Germany,
e-mail: fabricio.borges@ptb.de, markus.bartscher@ptb.de, michael.neugebauer@ptb.de

[2]Technical University of Denmark (DTU), Produktionstorvet Building 425, Room 209, 2800 Kgs. Lyngby, Denmark

e-mail: alesto@mek.dtu.dk

Abstract
The requirement of quality assurance of inner and outer structures in complex multi-material assemblies is one important factor that has encouraged the use of industrial X-ray computed tomography (CT). The application of CT as a coordinate measurement system (CMS) has opened up new challenges, typically associated with performance verification, specification definition and thus standardization. Especially when performing multi-material measurements, further, new, challenging effects are included in dimensional CT measurements, e.g. the influence of material A on material B in multi-material scenarios and the appropriate parameters for surface determination in a multi-surface setting. Thus, this paper presents – as part of a multi-material acceptance test and to create trust in multi-material CT measurement – a new concept for multi-material probing error testing (*P*-test) and discusses the test design and the first experimental results. This paper also attempts to perform a critical analysis of this new concept − featuring a compound sphere made of two half spheres of different materials − and tries to perform analyses of geometrical features of the new standard.

Keywords: Acceptance testing, Multi-material measurements, Computed tomography (CT), Standardization, Probing error test (*P*-test)

1 Introduction to probing error acceptance testing

Recently, the reliability of CT measurements has been of growing interest for several branches of industry. This growing interest is mainly driven by several advantages of CT over the conventional coordinate measurement systems (CMSs), which are mostly limited by physically accessible structures. In CT, this limitation is no longer present. In principle, CT is capable of measuring inner structures in complex workpieces as well as in complex multi-material workpieces or assemblies [1]. Although significant efforts have been devoted to trying to take CT-based CMSs to the same level of reliability as conventional CMSs (i.e. tactile and optical), CT has not yet achieved this level.

Basically, reliability might be achieved by means of assuring the traceability of a measurement technology. Traceability is assured by the evaluation of and statements on the measurement uncertainty associated with a specific measurement task. Thus, it relates the actual CT measurement to an international reference standard through an unbroken chain of calibrations. On the other hand, certain aspects of traceability can also be checked with regular performance verification using standardized test procedures, e.g. acceptance and reverification tests [2].

In the field of coordinate metrology, acceptance and reverification testing is the main topic of the well-established international ISO 10360 series of standards, currently focused on tactile and optical CMSs. In 2010, the ISO Technical Committee 213 Working Group 10 (ISO TC 213 WG 10) started to develop an ISO 10360 standard focused on acceptance and reverification testing for CT as a CMS [2]. But currently only the German national guideline (VDI/VDE 2630-1.3) published in 2011 is publically available [3].

According to all respective standards and guidelines in dimensional metrology, acceptance testing is a set of operations agreed upon by the CMS manufacturer and the user to check whether the CMS is performing according to the manufacturer's specifications. Thus, the test creates trust in the CMS, thereby helping to achieve traceability to the metre (the SI unit of length) for the measurands under test and it also tries to create comparability with CMSs adopting different sensor technologies. However, it should be kept in mind that acceptance testing does not provide complete traceability to the metre for arbitrary measurement tasks. As a consequence, the measurement uncertainty should be individually evaluated for each measurement task.

According to the ISO 10360 series, the main principle of acceptance testing is to perform an overall test of the entire performance of a CMS. Therefore, the test should be performed as an integrated system and it should assess the system using the complete measurement chain. The acceptance test should also reflect the standard use of the system and should cover all dominant errors affecting the CMS under study. Aspects of real-life objects (e.g. different X-ray penetration lengths) and for instance, the request for simple geometry reference standards in the test design should be taken into account while designing the test. Besides this, the difficulty to achieve comparability with other CMSs when using real-life objects and their complexity and variety limit the use of real-life objects in the scope of acceptance testing. Another important principle of acceptance

testing is to assess global and local performances of the error characteristics of a CMS. Global performance is assessed with a length measurement error test (*E*-test) by means of measuring (long) length reference standards (e.g. hole plates, step gauges, ball plates, etc.). Local performance – showing the ability to precisely locate the surface of a structure under test in a small spatial region – is assessed through a probing error test (*P*-test) by means of measuring the size and form of a (small) test sphere, see Figure 1. According to the German guideline VDI/VDE 2630-1.3 for dimensional CT, the test sphere should preferably have a diameter measuring from 0.1 to 0.2 times the diagonal of the field of measurement in the current magnification. According to the current ISO discussions on CT, four metrological quantities are under review for the mono-material *P*-test and ought to be compatible to the approach described in ISO 10360-8 for optical distance sensors [4]: *P*-test for form might be evaluated as *probing dispersion error* ($P_{\text{Form.Sph.D95\%::CT}}$) and *probing form error* ($P_{\text{Form.Sph.1x25::CT}}$); and *P*-test for size might be evaluated as *probing size error All* ($P_{\text{Size.Sph.All::CT}}$) and *probing size error* ($P_{\text{Size.Sph.1x25::CT}}$). These characteristics – to be measured at a test sphere – are to address the difficulty to achieve comparability with other CMSs when using real-life objects. Thus, this approach limits the complexity and variety in the scope of acceptance testing. According to the current discussions, the definition of the four metrological quantities of the *P*-test are given below:

1. **Probing dispersion error ($P_{\text{Form.Sph.D95\%::CT}}$),** the smallest possible width of all spherical shells that contains 95 % of all data points.
2. **Probing form error ($P_{\text{Form.Sph.1x25::CT}}$)**, the error of indication within the range of the Gaussian radial distance determined by an unconstrained least-square fit of 25 representative points on a test sphere
3. **Probing size error All ($P_{\text{Size.Sph.All::CT}}$),** the difference of the diameter of an unconstrained least-square fit of all points measured on a sphere and its calibrated diameter.
4. **Probing size error ($P_{\text{Size.Sph.1x25::CT}}$)**, the error of indication of the difference between the diameter of an unconstrained least-square fit of 25 representative points on a test sphere and its calibrated diameter.
5. **Remark on notation:** The above – in brackets – stated notation for the *P*-characteristics is deduced from the current evolution of standards in ISO 10360 (especially ISO 10360-8). It is in part described in [2], but is currently under development. There is no guarantee that the notation used here will be fully implemented in a first future ISO 10360 standard on mono-material CT specification and testing. The same statement needs to be made for the test itself. The final ISO 10360 mono-material *P*-test may differ from the above draft statements. The mono-material *P*-test characteristics serve only as a reference and are to enable the discussion of effects in this work for the multi-material case.

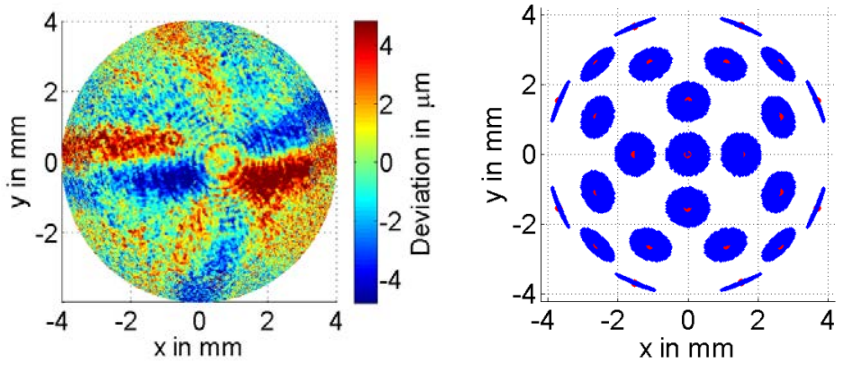

Figure 1. Probing error testing using a test sphere – a large number of points are evaluated. (a) Coloured error map of a sphere fit to the measured sphere data. Probing dispersion error using 95 % of the points, and probing size error All using all data points are deduced. (b) Probing error size and form evaluation using 25 representative points (given in red) based on 25 patches (given in blue) as a subset of all probed points (reproduced from [5])

$P_{\text{Form.Sph.1x25::CT}}$ and $P_{\text{Size.Sph.1x25::CT}}$ are determined by a least-square fit of 25 representative points on a test sphere. Representative points may be deduced from multiple point data inside an extended area – frequently called a patch – on the sphere. There is the constraint that the patch areas must not overlap. The concept of representative points has been introduced here – being first used in ISO 10360-8 – in order to achieve comparability between CT and tactile CMS measurements by reducing the impact of their influence factors such as noise for CT measurements and the size of the probing sphere of CMSs. However, a well-defined procedure on how to assess these characteristics in CT has not been finally established yet and is required to create an accepted testing scheme. This “uncertainty” has to be kept in mind when thinking forwards about potential multi-material acceptance tests.

The potential of CT in measuring multi-material components or assemblies has not yet been comprehensively explored, especially from the standardization point of view. Thus, what is common to all published guidelines and draft standards is that they all deal with the mono-material case [2, 6]. This means that the tests are not dedicated to making statements about the performance of CT-based CMSs when measuring multi-material objects. A further problem is that some of the proposed mono-material tests have a certain percentage of multi-material effects included [5]. Examples are mono-material reference

standards which are mounted on a different material. During testing, both materials are penetrated by X-rays and create effects with respect to the test measurand.
In this context, this work proposes for the first time a multi-material probing error test in the frame of acceptance testing. It also attempts to perform a critical analysis of this new concept − featuring a compound sphere made of two half spheres of different materials − and tries to perform analyses of geometrical features of the new standard.

2 Creating a multi-material probing test

This paper addresses one aspect of the challenge of creating a multi-material acceptance test for dimensional CT – specifically the multi-material probing error test. The multi-material length measurement error test (*E*-test) – as a second part which completes the multi-material acceptance test – is addressed in a further contribution to iCT2017 [7]. An important remark is that the whole multi-material acceptance test, consisting of a multi-material *P*-test and a multi-material *E*-test, is designed to complement –but not to substitute – the mono-material test!

2.1 Reference standards

The multi-material probing error test uses the accepted approach of the mono-material test performed with a "test sphere". In contrast to the mono-material case, the multi-material scenario comprises a compound test sphere consisting of two symmetric half spheres made of different materials. The two half spheres have (nominally) the same size and geometry. The half spheres are subsequently glued together using epoxy resin-based glue, see e.g. Figure 2. The intrinsic idea of this test is to assess the capability of a CT-based CMS to measure a small volume consisting of two different materials while a maximum compatibility of the new test to the accepted *P*-test in coordinate metrology is present.
In this work, mono- and multi-material spheres of a nominal size of 9/16 inches (about 14.3 mm in diameter) consisting of half spheres of different materials are used. The difference between the nominal diameter and the actual diameter and the difference between the single half sphere diameters are of the order of several micrometres. Three materials such as silicon nitride (Si_3N_4), aluminium oxide (Al_2O_3) and lead-free glass N-SF6 were paired, resulting in three multi-material compound spheres and – as a reference – three mono-material compound spheres. The materials were all selected due to their good mechanical proprieties and dimensional stability as well as their adequate X-ray attenuation coefficient ratios. The latter reflects the intention to analyse different test scenarios, where small and larger differences exist between the absorption coefficients. Table 1 presents the experimental attenuation coefficient ratios (μ_2/μ_1), at 150 kV X-ray tube voltage without using a physical filter on the tube. The attenuation coefficient is measured and calculated based on the well-known Lambert-Beer's Law and the X-ray transmission of each material quantified after a given penetration length. In Table 1, an attenuation coefficient ratio being close to 1, shows that the materials have a similar X-ray attenuation, whereas an attenuation coefficient ratio being close to 0, indicates that the materials are significantly different from an X-ray absorption point of view. Note that the values reported in the table are not physical constants because they depend upon the scanning parameters used. Thus, in the case studied here, N-SF6 absorption is larger than Si_3N_4 by a factor of 2.5. More asymmetric scenarios with respect to shape and absorption stay possible, e.g. reference object volumes of 5 % N-SF6 and 95 % Si_3N_4 as examples of an asymmetric shape or a reference object featuring half spheres made from steel and PEEK as an example of a more asymmetric absorption case, are in principle possible. The main focus of this work is however to test the new concept. Thus, extreme cases are not covered here. Besides this, the test should provide a compromise scenario between the (medium) worst and the easiest case scenarios.

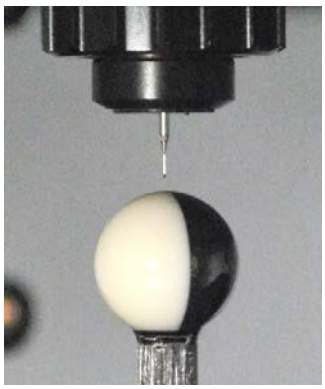

Figure 2. Example of a multi-material sphere, Al_2O_3 (white)/Si_3N_4 (black) multi-material sphere, assembled in a high precision tactile CMS

	Multi-material assembly of 2 half spheres			**Mono-material assembly of 2 half spheres**		
Materials (id_2/id_1)	Al_2O_3/Si_3N_4	Al_2O_3/N-SF6	Si_3N_4/N-SF6	Si_3N_4/Si_3N_4	Al_2O_3/Al_2O_3	N-SF6/N-SF6
Attenuation coeff. ratio (μ_2/μ_1) at 150 kV, no filter	0.9	0.5	0.4	1	1	1

Table 1. Material pairings used for the multi-material *P*-test realization and their X-ray attenuation coefficient ratio

The multi- and mono-material spheres were all calibrated using a tactile CMS. The calibration strategy is based on measuring the half spheres separately (but in the glued compound state). Two spheres are calculated from the probed points: half sphere material 1 (HS1), half sphere material 2 (HS2). An area of approximately 120° opening angle near the pole (i.e. opposite side of the carbon fibre shaft, see Figure 2) is covered by tactile points using a single point probing strategy. The expanded measurement uncertainty $U(k=2)$ of each single point was of the order of 1 µm or less. The gluing process of the multi-material half spheres was carried out manually; therefore, the gap caused by the glue is in the range of 40 µm to 150 µm. An area of approximately 500 µm near to the gap/glue area was thus excluded from tactile CMS probing. A total of 64 points evenly distributed on each half sphere – excluding the gap/glue area and its vicinity – were acquired. By this means, the glue/gap-related effects were excluded from the analyses. Diameter and form deviations of each half sphere as well as the distance between the centres of the two half spheres were finally determined. The form deviation for all the half spheres was found to be below 0.5 µm. This number is comparable to the specified form error of full spheres. Thus, it shows that cutting or grinding full spheres to create half spheres made of the given materials does not cause a significant degradation of the form. A good quality sphere shape is required in the test enabling a separation of effects. Half spheres with high form deviation (> voxel size) do not allow statements about multi-material effects due to the mixture of several influences present in the data. Therefore, the extent of the form errors is far smaller than the typical voxel sizes, ensuring that the impact of half spheres as reference standards, does not impair the conducted tests.

2.2 Experimental CT setups

The multi- and mono-material spheres considered within this work are listed in Table 1. Assemblies Si_3N_4/Al_2O_3, Al_2O_3/N-SF6 and Si_3N_4/N-SF6 include two half spheres made of different materials, while the remaining assemblies Si_3N_4/Si_3N_4, Al_2O_3/Al_2O_3 and N-SF6/N-SF6 comprise two half spheres of the same material.

For the CT scans used here, the spheres were all positioned with the glue/gap area parallel to the flat panel detector's centre column. However, further assembly set-ups need to be evaluated (e.g. glue/gap area 45° tilted to the flat panel detector's centre column). For the measurements, the PTB Nikon Metrology MCT225 system was used. All scans were performed with the same voxel size of (20 µm)[3]. A multi-sphere reference standard-based scaling correction was performed based on measurements before and after every CT scan to remove residual scaling errors, thus improving the accuracy of the measurement analysis of the proposed test. The stability of the scale between these reference scans was less than 0.2 µm over a length of 15 mm in all scans performed showing a favourable stability of the system. Scanning parameters, which are reported in Table 3, were selected for each assembly in such a way as to yield a similar noise level in the multi-material measurements but also to minimize beam hardening effects. The contrast-to-signal ratio (CNR) was used to evaluate the noise according to [8]. The CNRs of the multi- and mono-material scans in the reconstruction volume are presented in Table 2. The grey value profiles of the six multi- and mono-material CT scans are plotted in Figure 3-b and 3-c, respectively, and were obtained from the same slice of the different CT scans, as shown in Figure 3-a. The mono-material CT scans do not show a clear indication of the gap. It is worth noting that the above-mentioned choice of measurement parameters is driven by the need to analyse the proposed test itself. In an application of test, the test has to be conducted according to the manufacturer's given rated conditions and has to conform to the manufacturer's recommendations with respect to the measurement parameters.

CNR	N-SF6	Si_3N_4	Al_2O_3
N-SF6	17.2	23.3	23.3
Si_3N_4	7.8	23.8	25.8
Al_2O_3	7.8	24.2	25.1

Table 2. CNR in the multi-material probing CT scans, bold face entries in the table represent the materials where the CNR was calculated

	Voltage in kV	**Current in µA**	**Filter in mm**	**No. of projections**	**Exposure time in ms**	**Beam hardening correction[1]**	**Noise reduction[2] (reconstruction filter)**
Si_3N_4/Al_2O_3	200	46	0.25 Cu	1700	2000	None	Hanning/preset 2
Al_2O_3/N-SF6	220	55	1 Cu	1700	2829	Preset 2	Hanning/preset 2
Si_3N_4/N-SF6	220	55	1 Cu	1700	2829	Preset 2	Hanning/preset 2
Si_3N_4/Si_3N_4	200	46	0.25 Cu	1700	2000	None	Hanning/preset 2
Al_2O_3/Al_2O_3	200	46	0.25 Cu	1700	2000	None	Hanning/preset 2
N-SF6/N-SF6	220	55	1 Cu	1700	2829	Preset 2	Hanning/preset 2

Table 3. CT scanning parameters used for each assembly

[1] Nikon Metrology CT PRO 3D version 3.1.9 standard beam hardening correction based on a polynomial function of order 2 (preset 2) was carried out during the reconstruction of the projections.

[2] Nikon Metrology CT PRO 3D version 3.1.9 standard software-based noise reduction was carried out during the reconstruction of the projections. The settings applied to all of the assemblies evaluated were: filter type: Hanning; cut-off frequency: 100 % of maximum frequency; order: 1 and scaling: 1 were used (corresponding to preset 2 of software in use).

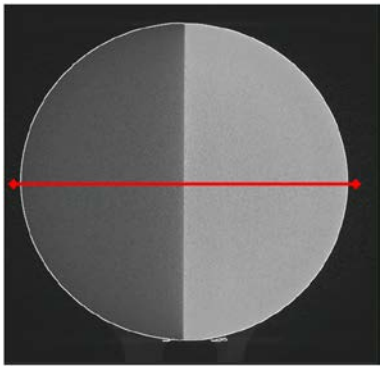

(a)

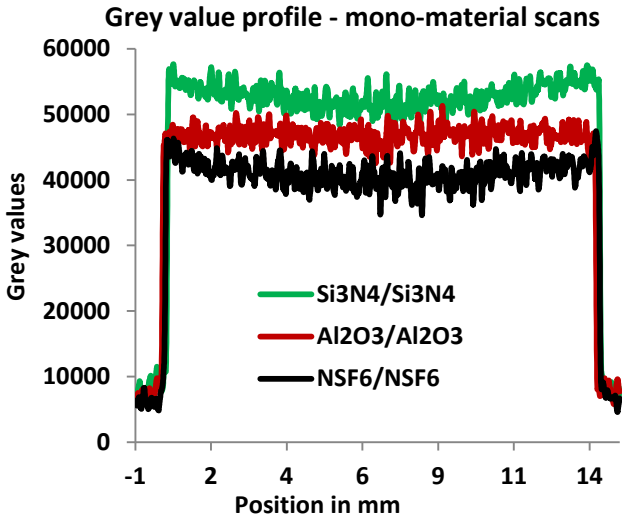

(b)

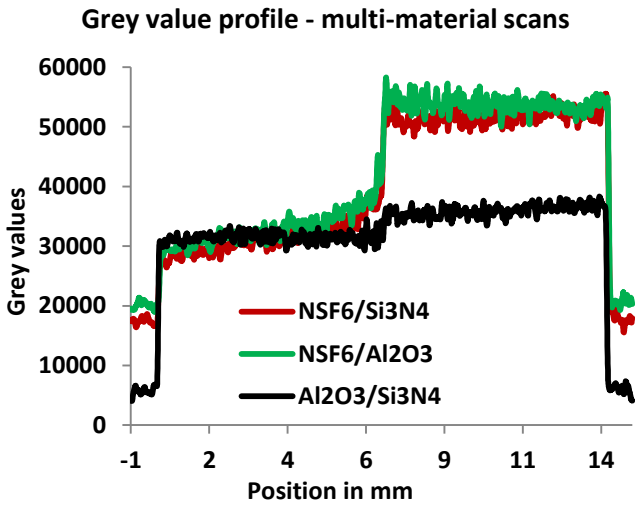

(c)

Figure 3. (a) Multi-material sphere assembly reconstruction CT slice, Si_3N_4 and N-SF6 as an example, with red line indicating horizontal profiles where the grey values (around 3200 points each) were extracted; (b) plot of the respective grey value profiles of the three mono-material scenarios; and (c) plot of the grey value profiles of the three multi-material scenarios

2.3 Evaluation

The evaluations of the multi-material influence on the probing error test (*P*-test) were based on the measurement deviations from the tactile reference measurements. Three measurands were considered within this work: the diameter and form of each half sphere (HS), and the distance between HS centres. The diameter and form characterize in-material measurands, while the distance between HS centres characterizes an inter-material measurand, see Figure 4. A simplified scheme of the workflow is presented in Figure 5 and it is performed as follows:

1. CT scans of the multi-material spheres and CT scans of the multi-sphere reference standard to allow scale correction scans before and after every CT scan of the multi-material spheres
2. Surface determination of the multi-material spheres – the surface determination of the multi-material spheres is first performed optimized for the low absorption material (LAM) and subsequently and independently for the high absorption material (HAM), separating them into two volumes
3. Fit spheres in the LAM volume half-sphere data and HAM volume half-sphere data and calculate the distance between their centres
4. CT data points are exported separately → LAM CT points; HAM CT points
5. Load CT data points into Matlab® application, developed at PTB[3]. For diameter and form deviation measurements, four main measurands are determined: Probing size error ($P_{\text{Size.Sph.1x25::CT}}$) and Probing size error All ($P_{\text{Size.Sph.All::CT}}$) for diameter, as well as Probing form error ($P_{\text{Form.Sph.1x25::CT}}$) and Probing dispersion error ($P_{\text{Form.Sph.D95\%::CT}}$) for form deviation. Details on how the patch operator is performed can be seen in [5]. The four *P*-test measurands are calculated for each half sphere separately.

[3] Matlab® application developed at PTB within the project "Examination of optical area 3D micro measuring methods", funded by the German BMWi Transfer Programme "Measuring, standardization, testing, quality assurance", support code VIIA5_5-12, 2012-2015.

Remark: Step 2 describes the procedure which has been used in this work. For final testing, an application conforming to the manufacturer's procedures is required.

The separate evaluation of two HSs differs from the standard mono-material *P*-test. However, this proposed multi-material test is additional to the standard test and it should be as efficient as possible avoiding redundant information. It is worth noting that for testing tactile CMSs, half spheres are always evaluated. For the case studied here, the information obtained at the separate HSs was shown to be sufficient for the analyses.

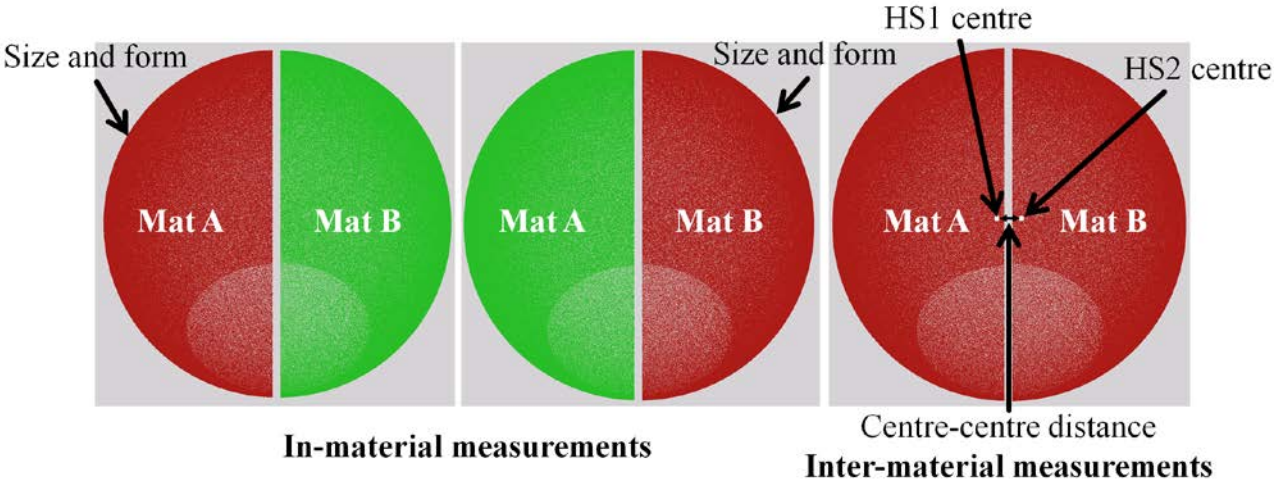

Figure 4. Measurement scenarios: in-material measurements in a multi-material scenario (creation of the elements for the measurand based on material A and air, material B and air, however, both materials A and B contribute to the total penetration length); inter-material measurements in multi-material scenario (creation of the elements for the measurand based on material A and air, material B and air)

Furthermore, when a complete sphere is calculated from the multi-material HSs, the measurand may comprise (non-desired) assembly-related effects which are also included in the test and which need to be tracked in the analysis.
The combined assembly-related effects, e.g. misalignment of an HS, lack of uniformity of glue thickness over the surface, etc., will be present in any realistic assembly; this means that the overall sphere geometry and size will be significantly impaired by the assembly effects in the µm range. Simulation-based preliminary studies of the assembly-related misalignments have shown a non-negligible influence on the results, unless data handling of an HS is applied, e.g. translation and rescaling of an HS relative to another HS. Furthermore, when the multi-material *P*-test is performed in a complete sphere scenario, some patches of the pattern should be excluded from the analysis, as they might comprise two different materials in a single patch. This patch scenario is not usual in coordinate metrology and it might be unfair when compared to the standard mono-material *P*-test. Besides this, the Feldkamp artefact (i.e. pole artefact) is also excluded in the approach applied in the multi-material *P*-test, as it is already included in the standard mono-material test. Therefore, in order to enable a fair test scenario for the probing error test in a multi-material assembled sphere, the HS data are evaluated separately. The same strategy was also applied to three mono-material spheres to check the concept.

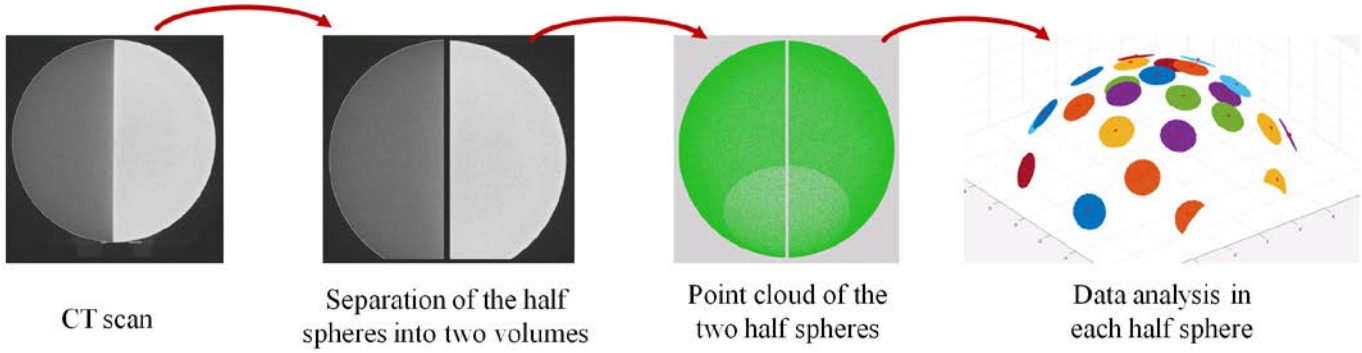

Figure 5. Workflow of the data analyses in this work including a final patch-based analysis

3 Results and conclusions

A multi-material probing testing scheme (*P*-test) in the scope of acceptance testing is presented for the first time in this work. The main objective of the work is to check whether there is an effect on form and size *P*-test measurements while performing multi-material measurements.

Thus, three multi- and three mono-material test spheres composed of two half spheres made of three different materials were scanned with CT. The evaluations of the multi-material spheres were based on deviations from tactile reference measurements. In every sphere assembly, each half sphere was evaluated separately, avoiding assembly/gluing related misalignments.
Probing size error ($P_{\text{Size.Sph.1x25::CT}}$) and Probing size error All ($P_{\text{Size.Sph.All::CT}}$) for diameter and Probing form error ($P_{\text{Form.Sph.1x25::CT}}$) and Probing dispersion error ($P_{\text{Form.Sph.D95\%::CT}}$), as currently discussed in the respective ISO standardization bodies for the mono-material *P*-test, were evaluated in this study for the multi-material case. The patch analysis concept which has been applied to Probing form error ($P_{\text{Form.Sph.1x25::CT}}$) and Probing size error ($P_{\text{Size.Sph.1x25::CT}}$) has been deduced from the approach from ISO 10360-8 and is also being discussed at ISO for the mono-material *P*-test case. Additionally, the distances between the half sphere centres were also evaluated, in order to investigate in total whether there is a multi-material effect on the form deviation, the size and the distance of the half spheres.
The results of this new mono- and multi-material *P*-test for size and form are presented in Figure 6. Besides this, the half sphere distances (centre-to-centre distance) evaluated in this study can also be seen in Figure 6.
In general, a significant multi-material effect on the form measurements can be observed. Figure 6-b shows a larger probing dispersion error ($P_{\text{Form.Sph.D95\%::CT}}$) for Si_3N_4 and Al_2O_3 when scanned together with N-SF6. $P_{\text{Form.Sph.D95\%::CT}}$ appears to be more influenced by the material effects than all other probing characteristics, see Figure 6-a where there is a slight increase of the form deviation for higher absorption materials. However, no significant multi-material effect on $P_{\text{Form.Sph.1x25::CT}}$, *P*-test size and distance was observed. This is especially true when considering the voxel size of $(20\ \mu m)^3$. All errors assessed here are below one voxel size. Thus, effects below 10 % of the voxel size do not appear to be significant and reflect – to some extent – the uncertainty of the study.
The proposed multi-material probing testing scheme was successfully evaluated, and multi-material-related effects were observed in the $P_{\text{Form.Sph.D95\%::CT}}$ probing characteristics. Further studies are still however possible. For instance, a more challenging multi-material scenario may be used, e.g. PEEK (plastics) and Fe (metal), once the maximum attenuation coefficient difference between two materials is 60 % for Si_3N_4 and N-SF6, cf. Table 1.

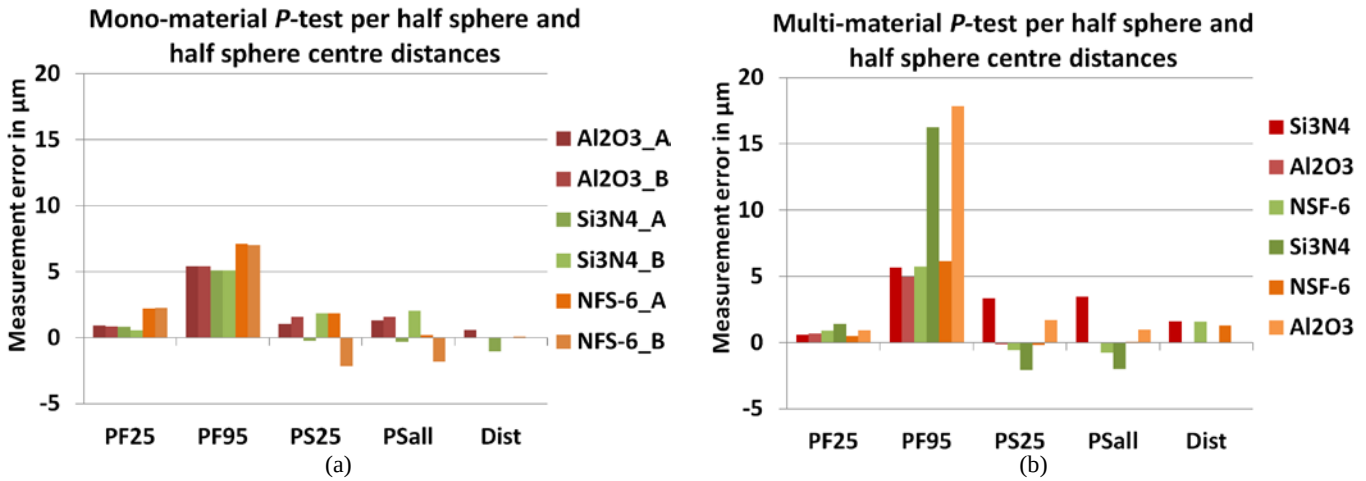

Figure 6. CT scan results of mono-material probing testing (a) and multi-material probing testing (b); simplified notation of the *P*-test characteristics: PF25 = $P_{\text{Form.Sph.1x25::CT}}$, PF95 = $P_{\text{Form.Sph.D95\%::CT}}$, PS25 = $P_{\text{Size.Sph.1x25::CT}}$, and PSall = $P_{\text{Size.Sph.All::CT}}$

Acknowledgements

We would like to thank the EU Marie Curie Initial Training Networks (ITN) − INTERAQCT, grant agreement no.: 607817, for the project funding. More information can be seen at http//:www.interaqct.eu.
We would also like to express our gratitude to our colleagues Karsten Kusch, PTB, for gluing the half spheres, along with Jakob Schlie, PTB, for the reference measurements of the multi-material spheres and for the patch-based probing test analysis application.

References

[1] L. De Chiffre, S. Carmignato, J.-P. Kruth, R. Schmitt, and A. Weckenmann, Industrial applications of computed tomography, CIRP Annals - Manufacturing Technology, vol. 63, no. 2, pp. 655–677, 2014.
[2] M. Bartscher, O. Sato, F. Härtig, and U. Neuschaefer-Rube, Current state of standardization in the field of dimensional computed tomography, Measurement Science and Technology, vol. 25, no. 6, p. 064013, 2014.
[3] VDI/VDE 2617/2630 - Part 13/Part 1.3 (2011). Guideline for the application of DIN EN ISO 10360 for Coordinate Measurement Machines with CT sensors. VDI, Duesseldorf, 2011.
[4] ISO 10360-8:2013 Geometrical product specifications (GPS) - Acceptance and reverification tests for coordinate measuring systems (CMS) – Part 8: CMMs with optical distance sensors. International Organization for Standardization, Geneva.

[5] F. Borges de Oliveira, M. Bartscher, and U. Neuschaefer-Rube, Analysis of combined probing measurement error and length measurement error test for acceptance testing in dimensional computed tomography. Digital Industrial Radiology and Computed Tomography (DIR 2015), University of Ghent, Ghent, 22-25 June 2015, available as http://www.ndt.net/events/DIR2015/app/content/Paper/31_BorgesdeOliveira.pdf
[6] M. Bartscher, J. Illemann, and U Neuschaefer-Rube, ISO test survey on material influence in dimensional computed tomography, Case Studies in Nondestructive Testing and Evaluation, Volume 6, Part B, Pages 79–92, November 2016, http://dx.doi.org/10.1016/j.csndt.2016.04.001
[7] F. Borges de Oliveira, M. Bartscher, U. Neuschaefer-Rube, R. Tutsch, and J. Hiller, Creating a multi-material length measurement error test for the acceptance testing of dimensional computed tomography systems, KU Leuven, Leuven iCT 2017, 07-09 February 2017, to be published.
[8] K. M. Hanson, Detectability in computed tomographic images, Medical Physics 6(5), (1979) pp 441-451.